www.czasopisma.pan.pl PAN POLSKA AKADEMIA NAUK www.journals.pan.pl

Arch. Metall. Mater. **68** (2023), 3, 1183-1189

DOI: https://doi.org/10.24425/amm.2023.145492

J. MORGIEL[1*], T. DUDZIAK[2], L. MAJ[1], A. KIRCHNER[3], M. POMORSKA[1], B. KLÖDEN[3], T. WEISSGÄRBER[3], D. TOBOŁA[2]

ROLE OF NITROGEN DURING DRY-AIR OXIDATION OF TiAlNbCrSi ALLOY PRODUCED WITH MOULD CASTING (MC) AND ELECTRON BEAM MELTING (EBM)

The lack of room-temperature ductility of high-strength TiAl-based alloys called for complicated high temperature processing limiting their application areas. Introduction of additive manufacturing (AM) methods allowed to circumvent this disadvantage, but entailed microstructure refinement affecting, among the others, their oxidation resistance. The dry-air high temperature oxidation processing of TiAl-based alloys is relatively well covered for coarse grained materials, but to what extent the TiAl alloys are affected by the changes caused by the AM remains to be found out. Additionally, the role of nitrogen during these processes was to large extent omitted in previous works. Within the present experiment, the mould cast (MC) and the electron beam melted (EBM) Ti-48Al-2Nb-0.7Cr-0.3Si (at. %) RNT650 alloys were dry-air oxidized at 650°C for 1000 h. The TEM/EDS investigations allowed to confirm that the scale formed during such treatment consists of the layers occupied predominantly by TiO_2+Al_2O_3/TiO_2/Al_2O_3 sequence. Additionally, it was shown that N diffuses to the sub-scale and reacts with the substrate forming two distinct discontinuous sub-layers of α_2-Ti_3Al(N) and TiN. The scale over EBM was noticeably less porous and nitrogen penetration of the substrate was more extensive, while the MC showed higher susceptibility to local sub-scale oxidation.

Keywords: TiAlNbCrSi; dry-air oxidation; TiN; TEM

1. Introduction

The TiAl-based alloys are characterized by low weight and high strength retained within a wide temperature range. However, an inherent brittleness of these materials makes their processing with standard metallurgical industry techniques extremely demanding. The above situation limits their wider applications for high-cost products like parts of car engines or aircraft turbines [1,2]. Nevertheless, the development and following fast progress observed in recent years of various industrially implemented additive manufacturing techniques could make a real break-through toward wider use of these materials [3-5].

The change of processing route of TiAl-based alloys from originally used mould casting (MC) and hot forging toward an additive manufacturing one involving electron beam melting (EBM), entails a strong modification of the product microstructure, i.e. from a fully lamellar (γ-FL) to a nearly lamellar (γ-NL) or locally even to a duplex equiaxed mixture of α_2-Ti_3Al and γ-TiAl [2]. Such a change only slightly compromises creep and strength of these alloys, but simultaneous microstructure refinement might also decrease their high temperature oxidation resistance which, aside of nearly total lack of ductility, was the other week spot of these materials [6]. Fortunately, the elaborated for EBM processing low shrinkage RNT650 Ti-48Al-2Nb-0.7Cr-0.3Si (at. %) alloy showed only slightly higher mass gain in oxidizing atmospheres at 650°C in comparison to the same alloy produced by centrifugal MC method [7]. This generally positive outcome means that an effect of changing a way of processing on the scale growth under these conditions should be relatively minor, but having in mind a sensitive character of eventual aviation application, it has to be fully assessed anyway.

Practically, all proposed dry-air oxidation mechanisms for the TiAl-based alloys produced using standard metallurgical processing ways pointed to formation of a scale built of TiO_2 + Al_2O_3 / TiO_2 / Al_2O_3 sequence of layers [8], which was confirmed also for the EBM manufactured material [7]. However, it involves only the elements playing major role during the scale

[1] POLISH ACADEMY OF SCIENCE, INSTITUTE OF METALLURGY AND MATERIALS SCIENCE, 25 REYMONTA STR., 30-059-KRAKÓW, POLAND
[2] ŁUKASIEWICZ RESEARCH NETWORK, KRAKÓW INSTITUTE OF TECHNOLOGY, 73 ZAKOPIANSKA STR., 30-418 KRAKÓW, POLAND
[3] FRAUNHOFER-INSTITUT FÜR FERTIGUNGSTECHNIK UND ANGEWANDTE MATERIALFORSCHUNG IFAM, INSTITUTSTEIL DRESDEN WINTERBERGSTRASSE 28, 01277 DRESDEN, GERMANY

* Corresponding author: j.morgiel@imim.pl

development, while the nitrogen being the only other element present in larger amounts during dry-air oxidation was routinely omitted in this consideration. This situation persisted even as already in the nineties Dettenvanger [9] and Lang [10] suggested that the so called "nitrogen effect" is responsible for inability to form a continuous alumina layer over these alloys, i.e. that during nucleation stage TiN is successfully competing with Al_2O_3, but later is oxidized into TiO_2 contributing to the scale porosity. However, up till now the active role of nitrogen during dry-air oxidation of the TiAl-based alloys was confirmed only for later stages of this process by development of thick layers of TiN and Ti_2AlN phases in the sub-scale areas.

Therefore, the present work was aimed at assessment of nitrogen distribution during the early stage of the dry-air scale formation over the RNT650 Ti-48Al-2Nb-0.7Cr-0.3Si alloy. The microstructure of the investigated material was characterized using the transmission electron microscopy (TEM) method, while measurements of local chemical composition were carried out with energy dispersive spectroscopy (TEM/EDS) attachment.

2. Experimental procedure

The centrifugal mould cast (MC) and electron beam melted (EBM) Ti-48Al-2Nb-0.7Cr-0.3Si (at. %) RNT650 alloys were acquired in the form of rods (ϕ ~13 mm). The samples were cut into 3 mm discs, cleaned and subjected to dry-air oxidizing atmosphere at 650°C for 1000 h. The other experimental details concerning sample cleaning, oxidation stand as well as applied treatment were given in our previous work [7].

The microstructure investigations were performed with FEI Tecnai G2 SuperTWIN FEG (200 kV) and probe corrected ThermoFisher Themis (200 kV) transmission electron microscopes (TEM) equipped with windowless 4 quadrant Super-X energy dispersive spectroscopy (EDS). The maps built of 500 × 500 pixels (0.5 nm electron probe) and profiles (each step being a sum of the intensity of 25 pixels strung perpendicular to profile line) were acquired to document a distribution of the alloying elements. The above information was filtered from the background by using "net counts", what helped to minimize the overlap of the neighbouring lines of N, O and soft X-ray radiation from Ti (Ti-La lines). The thin foils for these experiments were prepared with the focused ion beam (FIB) method using ThermoFisher Scios 2 Dual Beam system. Up to three layers of carbon of overall thickness approaching 500 nm were deposited on the scale surface securing a proper contrast of fine surface features.

3. Results

The MC Ti-48Al-2Nb-0.7Cr-0.3Si was characterized by coarse grain microstructure filled with sets of parallel α_2-Ti_3Al / γ-TiAl lamellas, i.e. fully lamellar (FL) one (Fig. 1a). Its oxidation in dry-air at 650°C resulted in the development of the scale filled with roughly equiaxed nano-crystallites (Fig. 1b). The scale surface was overgrown with only slightly larger thin hexagonal platelets and stubby rods, while discontinuous strings of larger voids were located at its centre. At the scale bottom, the material was very porous forming a kind of mushy zone. The scale/substrate boundary was usually cutting lamellas perpendicularly to its length propagating in a step-like manner. It is notable that the tips of the lamella extending toward the scale are more defected (or carry some precipitates) than the parts staying farther away from it.

The EBM alloy microstructure was of much more refined character that the MC one, it resembled rather that characteristic for the nearly-lamellar (γ-NL) or even duplex (D) one with the presence of micro-colonies of α_2-Ti_3Al / γ-TiAl platelets intermixed with smaller equiaxed grains of γ-TiAl (Fig. 2a). The presence of TiSi and Cr rich precipitates among them was also noted. The scale grown over this alloy under the same oxidizing environment was of comparable thickness and built generally along the same scheme. The only difference was that in this case it was free of larger voids in its middle part (Fig. 2b). The scale / substrate interface was of more flattened character as the oxidation front interacted with relatively fine grain material.

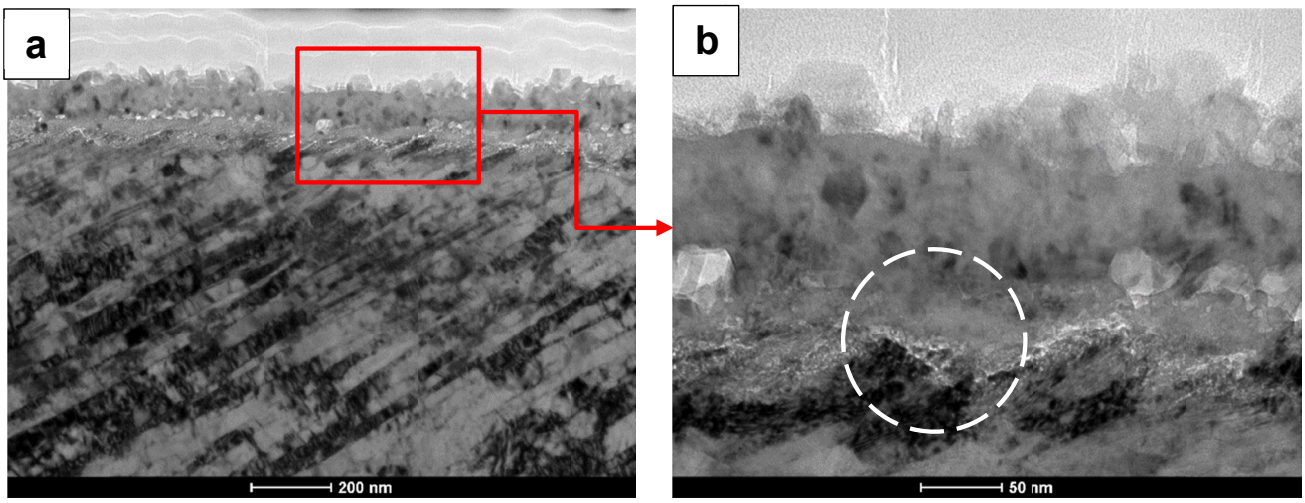

Fig. 1. TEM/ BF microstructure images presenting overview of dry-air oxidized MC near surface area (a) and details of scale/substrate boundary (b)

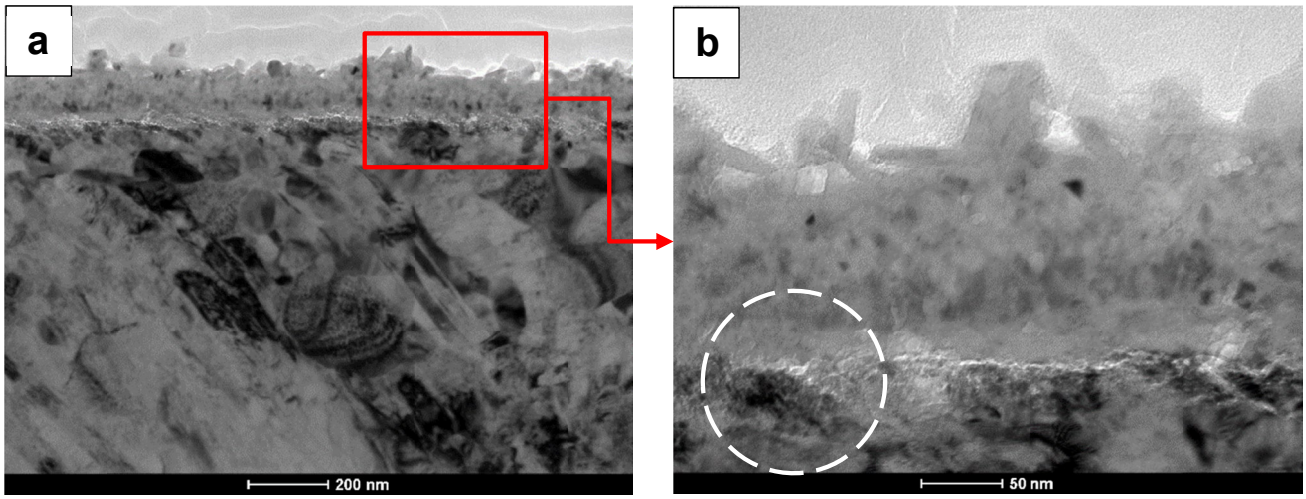

Fig. 2. TEM/BF microstructure images presenting overview of dry-air oxidized EBM near surface area (a) and details of scale/substrate boundary (b)

The latter feature made an assessment of the effect of the applied treatment on the sub-scale substrate areas problematic, as an eventual newly nucleated and grown crystallites in this area were impossible to distinguish from those being part of original duplex microstructure. The electron diffraction patterns acquired from the sub-scale area of both the MC and EBM alloys showed the presence of numerous fine spots (Fig. 3). Those which were strung around rings gave a good match with α-Al_2O_3 phase, while others grouped in a regular net corresponding to sections of the reciprocal lattice of the TiN phase (see inserts in Fig. 3a, b).

The assessment of a local chemical composition of the scale built during dry-air oxidation of the Ti-48Al-2Nb-0.7Cr-0.3Si alloy using TEM/EDS method has to take into account close location or even overlap of the lines representing nitrogen, oxygen and titanium as well as that of carbon (the last one used during FIB sample preparation), as shown in the EDS spectra given in Fig. 4. Therefore, the raw counts used for presenting maps of local distribution of N are to large extent a superposition of those generated using energy window ascribed to Ti-Lα, O and C (Fig. 5a). However, using net counts, i.e. with the background cut off allows to filter the information from each element and obtain maps presenting their real distribution (Fig. 5b). The above procedure causes a simultaneous strong diminishing of number of counts ascribed to each pixel (most visible in areas practically void of this element). The above procedure is also very efficient as it touches analysis of titanium distribution in this material, even if the position of its main L line (Ti-Lα) lies close to O-K line. Therefore, the map built of raw "Ti-L" counts presents practically superimposed distribution of the Ti, N and O, but that built of net "Ti-L" counts shows the properly filtered information, i.e. exactly like the one produced using free from any overlapping Ti-K (Ti-Kα) line (compare respective maps in Fig. 6). Simultaneously, there is no advantage of using net counts over the raw ones for building map from peak separated from the others, like in case of Ti-Kα.

The EDS maps presenting local chemical composition of the oxidized MC alloy built solely of the net counts of lines of respective elements showed that the scale was characterized by layered structure. Its upper part consisted predominantly of mixture of TiO_2 and Al_2O_3, centre of TiO_2 and the bottom of Al_2O_3 (Fig. 7).

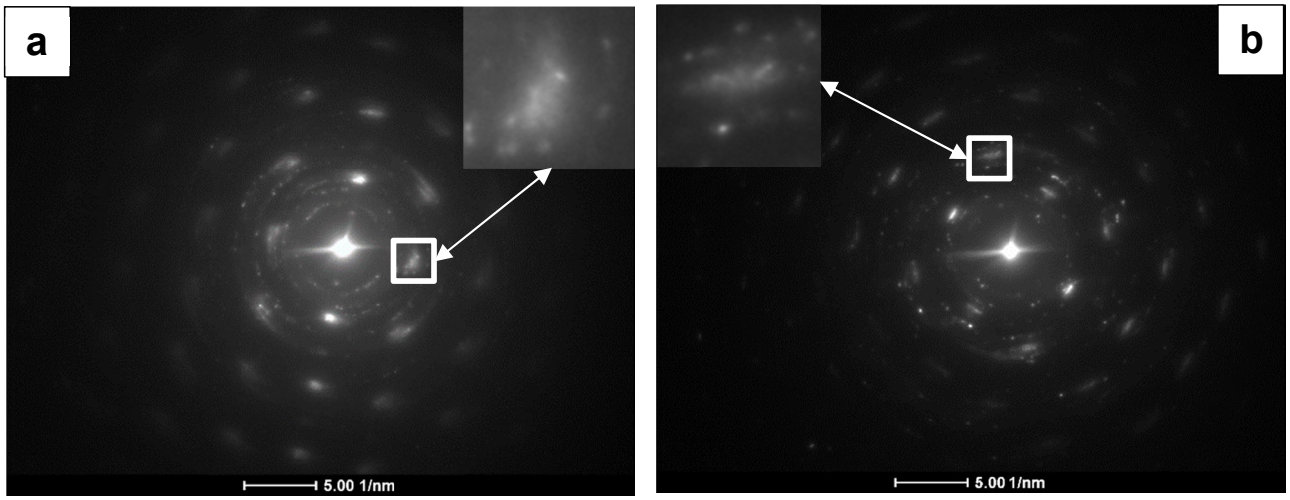

Fig. 3. TEM/SA diffraction patterns acquired from subscale area of MC (a) and EBM (b) alloys from areas marked with broken circles in Fig. 1b and 2b respectively (inserts present enlarge spot forming regular net)

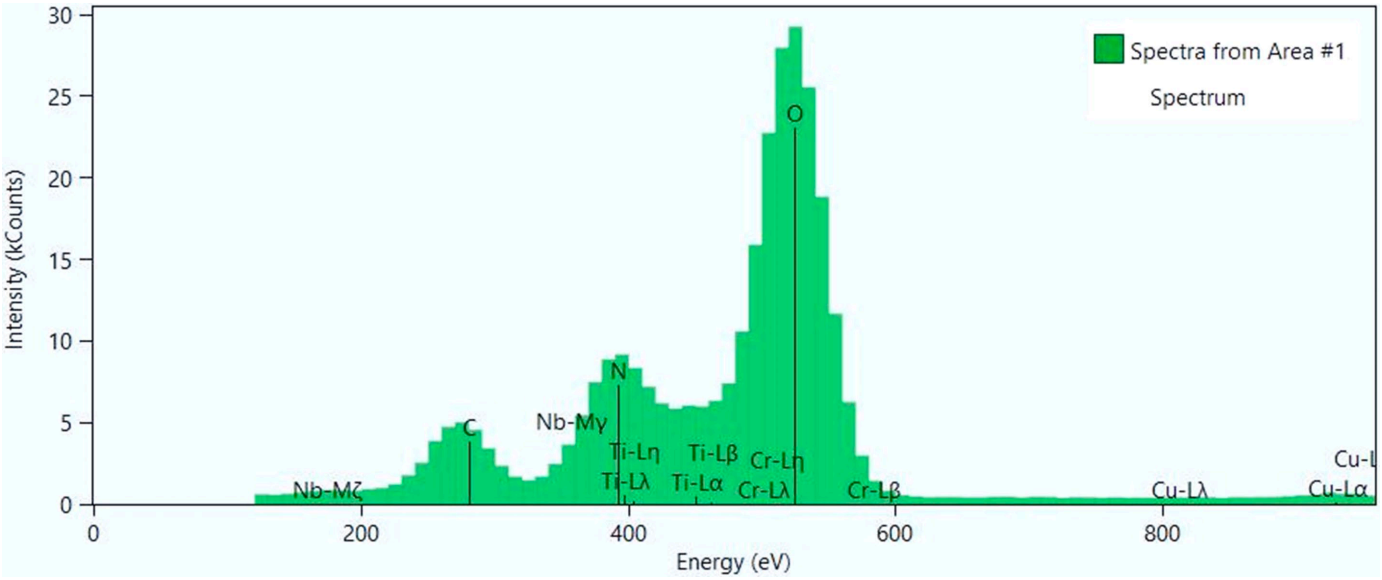

Fig. 4. Part of EDS spectra acquired from the bottom part of the scale formed on MC alloy

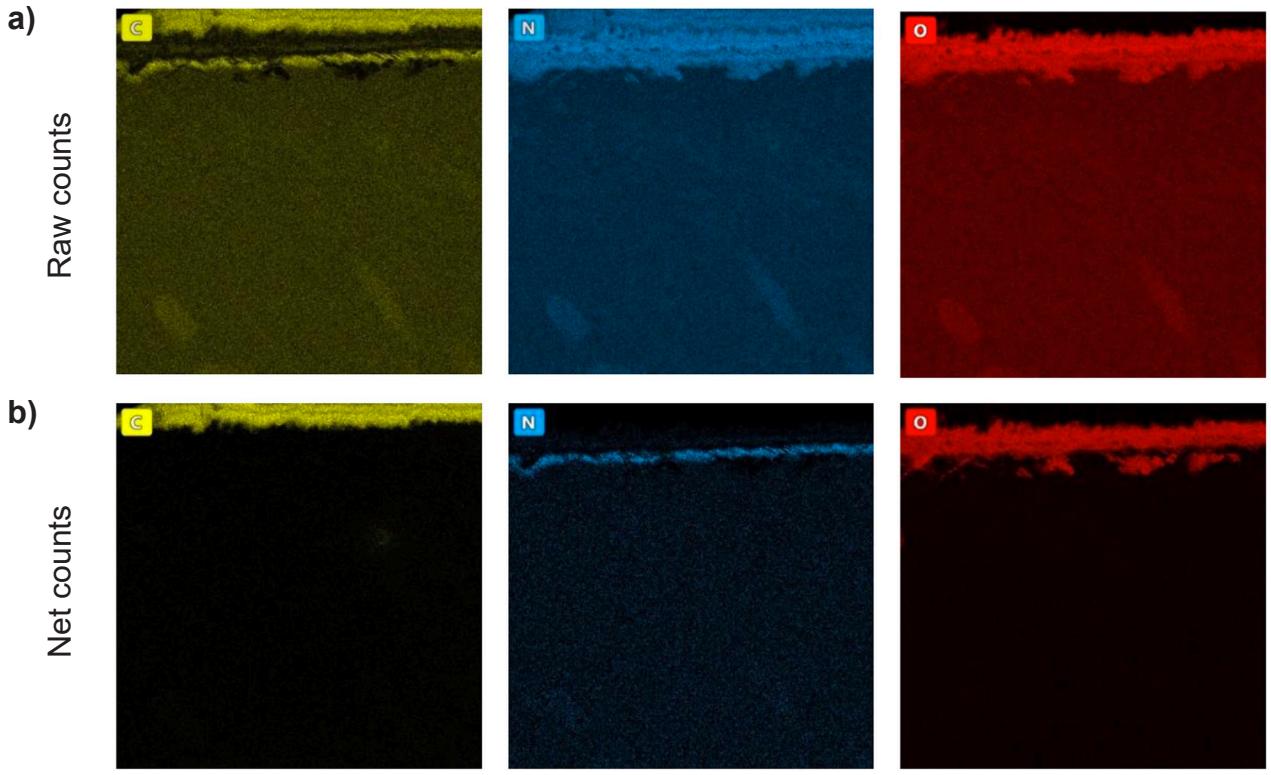

Fig. 5. EDS maps presenting distribution of C, N and O in scale and its vicinity built using: a) raw counts and b) net counts

Only below the oxide scale the presence of a thin but distinctive N enriched layer was noted. The same measurements done for the scale formed over the EBM alloy showed that it was stratified in similar way (Fig. 8). The profiles taken along the lines marked on composite N+O maps helped to establish that within the top layer of both scales the ratio of rutile to alumina is approx. 1:2. Additionally, the N concentration accumulated under the scale developed on the EBM material is evidently stepped suggesting the presence of two phases differing in N concentration. The layer with the lower N level contains roughly as much Ti and Al as found in the α_2-Ti_3Al lamellas located deeper in the substrate. It means that this layer may be formed by α_2-$Ti_3Al(N)$ phase. In such case the one above with higher content of N and Ti might be only formed by TiN (possible with remnants of TiAl).

4. Discussion

The research on the TiAl-based alloys resistance to the surface degradation caused by the exposure to air at high

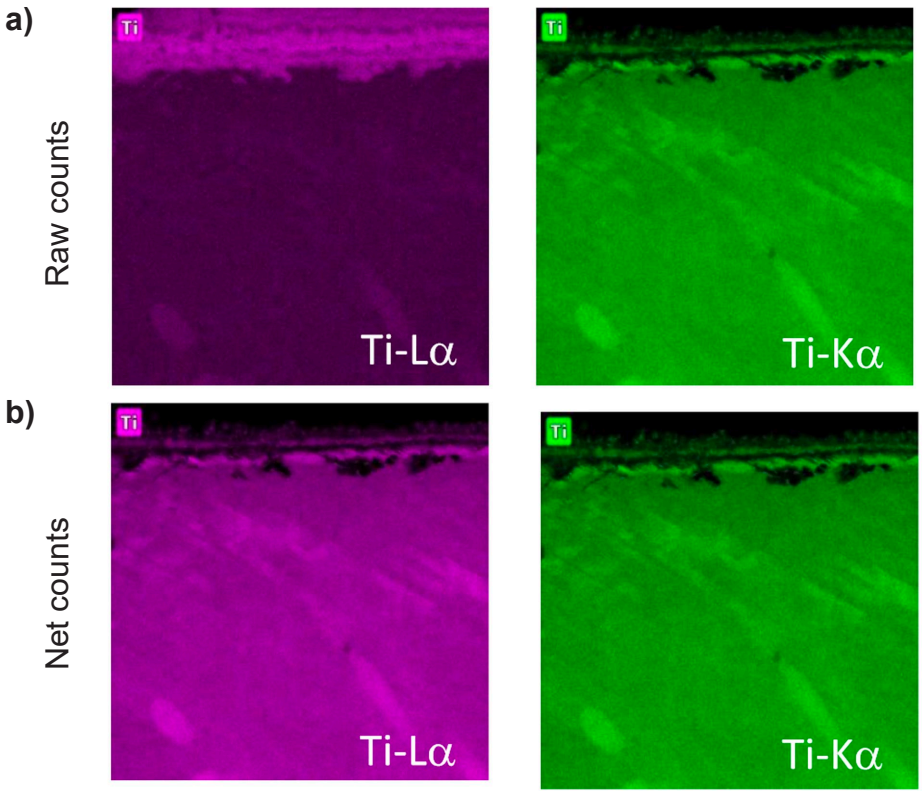

Fig. 6. EDS maps presenting distribution of Ti in scale and its vicinity built using: a) raw counts and b) net counts of Ti-Lα and Ti-Kα lines

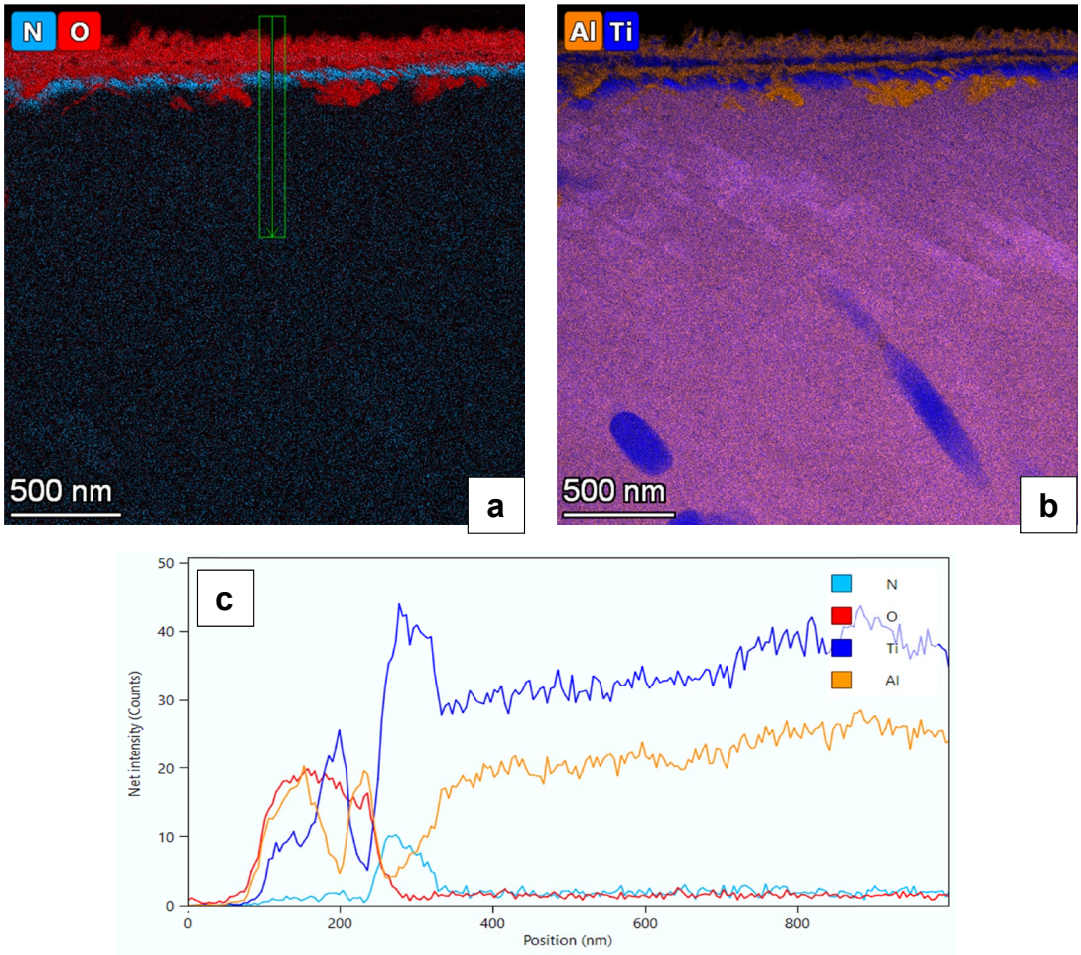

Fig. 7. EDS composite maps presenting distribution of superimposed signals from N+O (a), Ti+Al (b) and adjoining concentration profile acquired along line marked on N+O map (c)

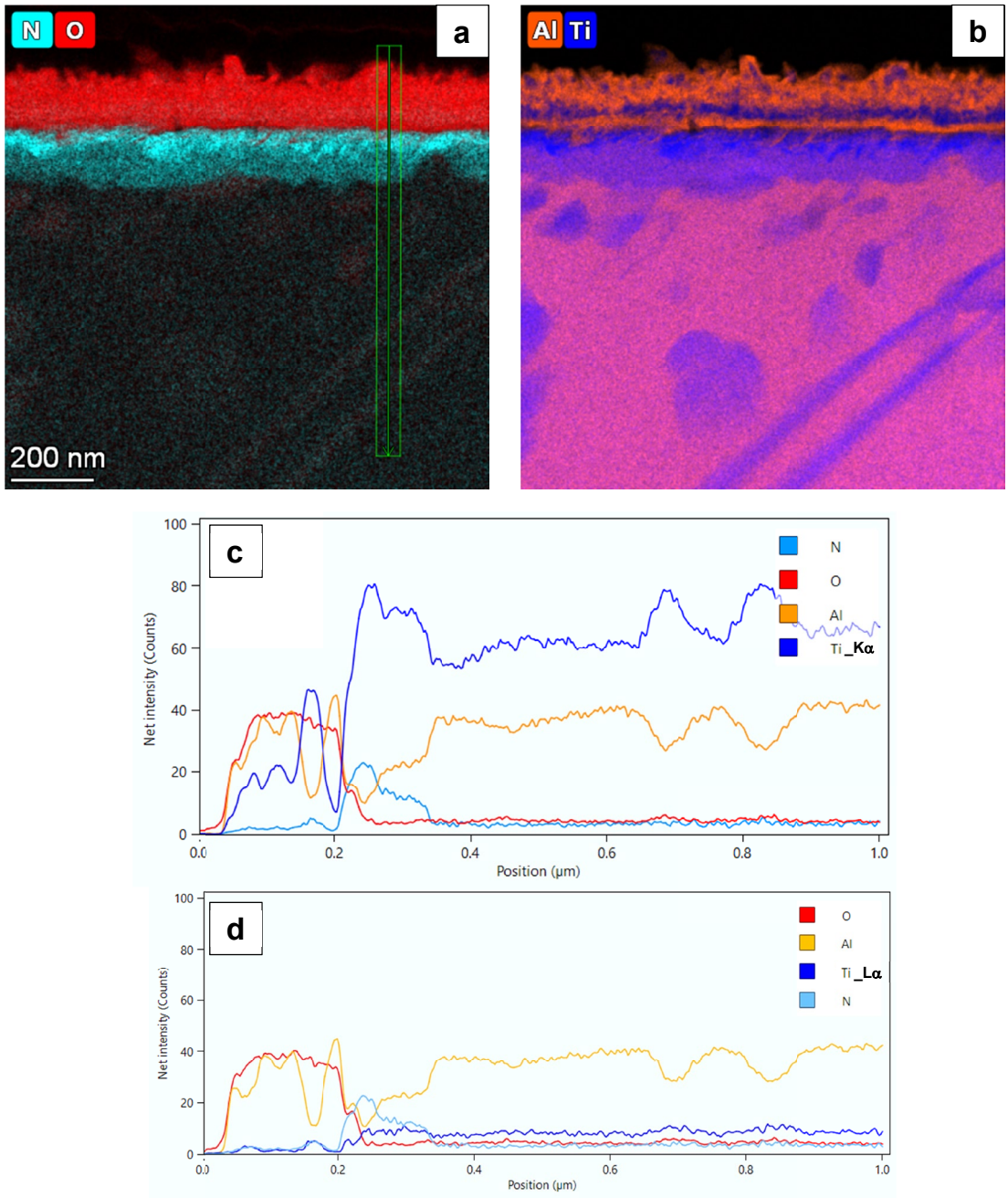

Fig. 8. EDS composite maps presenting distribution of superimposed signals from N+O (a) and Ti+Al (b), as well as adjoining concentration profiles (acquired along line marked on N+O map) acquired with Ti-Kα (c) and Ti-Lα lines (d)

temperature, simulating their working environment, was usually limited to the assessment of the oxidation processes [6-8], which in this case were quite complicated by themselves. The eventual reaction with nitrogen was usually skipped as of lesser importance and hampered by the problems with determination of a distribution of this element within the scale rich both in titanium and oxygen. The TEM/EDS method allowing to build maps with the raw counts produced in case of this material usually gave practically the same results for the N, O and Ti-Lα, as it was presented in Fig. 5. The raw counts use was a must in the case of less efficient X-ray EDS detectors of previous generation (small active area/ mylar window/ necessity to tilt thin foil toward detector). In contrast, a new four element detectors, like the SuperX EDS on Themis microscope, allow to work with the net counts capable of differentiating all these elements at still acceptable signal to noise ratio. Validity of this approach is separately confirmed through the possibility to generate exactly the same map of distribution of titanium with T-Lα as with the Ti-Kα line (Fig. 6).

Examining the nitrogen distribution in the dry-air oxidized MC and EBM Ti-48Al-2Nb-0.7Cr-0.3Si alloys using the discussed above TEM/EDS approach showed that it was the sub-scale area, which carried more significant amount of this element. It agrees with other measurements pinpointing the presence of N below oxides grown over air oxidized material like those performed with Auger Electron Spectroscopy (AES)

[11] or TEM/EDS [12,13], even if they were performed on much thicker scales representing late oxidation stages. Notable, in case of the EBM alloy the nitrogen concentration profile was stepped suggesting possibility of the presence of two phases in that area. Taking as a reference the intensity of the Ti-Kα line from the α_2-Ti_3Al lamellas located deeper in the substrate (Fig. 8), one may claim that the layer characterized by lower nitrogen level might represent α_2-$Ti_3Al(N)$ phase. Consequently, the layer with higher nitrogen content should be ascribed to the TiN, especially as electron diffractions acquired from those areas gave a good correspondence with such a phase. Within the scale also nitrogen was present in much lesser amount forming small enrichments linked to the layers with larger portions of TiO_2 (Fig. 8d).

5. Summary

The detailed TEM/EDS characterization of the scale formed over the MC and EBM Ti-48Al-2Nb-0.7Cr-0.3Si alloys after exposure to dry-air at high temperature helped to establish that during this treatment the nitrogen along with the oxygen diffuses to the reaction front with the substrate.

After arrival to the reaction front, the nitrogen firstly dissolves in the sub-scale parts of γ-TiAl/ α_2-Ti_3Al promoting its transformation into a single α_2-$Ti_3Al(N)$ phase. Secondly, continuing influx of nitrogen into these areas stimulates nucleation and growth of the TiN one. The oxygen acts in more local way by infiltrating the substrate in-between the nitrogen islands. In these places it forms a deep pocket (in case of coarse fully lamellar MC alloy) and finer channels (in case of fine crystalline EBM alloy) both filled with amorphous alumina. Simultaneously, the incoming O flux slowly oxidizes the newly developed TiN layer, while freed N along with incoming flux of this element from the gas atmosphere promote nitriding of still lower areas of the substrate, like it was presumed previously by examination of thick scales, i.e. late oxidation stages [11-13].

The oxidation process of the multicomponent TiAl-based alloys, like the Ti-48Al-2Nb-0.7Cr-0.3Si one is a complicated one and its full understanding has to take into account also the activity of the minor alloying additions like Nb, Cr and Si, which were specially introduced to modify it. However, interactions between the main alloying additions with the oxygen and nitrogen are the key issue in this process, especially as the role of the latter turned out to be more significant than it was originally thought.

REFERENCES

[1] F.D. Fisher, Deformation mechanisms in TiAl intermetallics – experiment and modelling, Proceedings of Mechanics of Advanced Materials 43-84, MAN'2001.

[2] P.V. Cobbinah, W.R. Matizamhuka, Review Article: Solid-State Processing Route, Mechanical Behaviour, and Oxidation Resistance of TiAl Alloys, Advances in Materials Science and Engineering 4251953 (2019).

[3] M. Thomas, M.P. Bacos, Processing and Characterization of TiAl-based Alloys: Towards an Industrial Scale, ONERA Journal Aerospace Lab, Alain Appriou **3**, 1-11 (2011).

[4] W.E. Frazier, Metal Additive Manufacturing: A Review, Journal of Materials Engineering and Performance **23**, 1917-1928 (2014).

[5] A. Emiralioglu, R. Unal, Additive manufacturing of gamma titanium aluminide alloys: A review, Journal Materials Science **57**, 4441-4466 (2022).

[6] J. Dai, J. Zhu, Ch. Chen, F. Weng, High temperature oxidation behaviour and research status of modifications on improving high temperature oxidation resistance of titanium alloys and titanium aluminides: A review, Journal of Alloys and Compounds **686**, 784-798 (2016).

[7] T. Dudziak, E. Rząd, J. Morgiel, M. Wytrwal-Sarna, A. Kirchner, M. Pomorska, T. Polczyk, G. Moskal, D. Toboła, B. Klöden, T. Weißgärber, Effect of fabrication process on oxide morphology and structure developed in rich oxygen atmospheres using electron beam melted and cast Ti-48Al-2Nb-0.7Cr-0.3Si alloys, Intermetallics **145**, 107553 (2022).

[8] S.A. Kekare, P.B. Aswath, Oxidation of TiAl-based intermetallics, Journal of Materials Science **32**, 2485-2499 (1997).

[9] F. Dettenwanger, E. Schumann, M. Ruehle, J. Rakowski, G.H. Meier, Microstructural Study of Oxidized γ-TiAl, Oxidation of Metals **50**, 269-307 (1998).

[10] C. Lang, M. Schutze, TEM investigations of the early stages of TiAl oxidation, Oxidation of Metals **46**, 255-285 (1996).

[11] G. Meier, F. Pettit, S. Hu. Oxidation behaviour of titanium aluminides. Journal de Physique IV Proceedings, EDP Sciences **3**, 395-402 (1993).

[12] W. Lu, C.L. Chen, L.L. He, F.H. Wang, J.P. Lin, G.L. Chen, (S) TEM study of different stages of Ti–45Al–8Nb–0.2W–0.2B–0.02Y alloy oxidation at 900°C, Corrosion Science **50**, 978-988 (2008) .

[13] J. Hui-ren, W. Zhong-lei, M. Wen-shuai, F. Xiao-ran, D. Ziqiang, Z. Liang, L. Yong, Effects of Nb and Si on high temperature oxidation of TiAl, Transactions of Nonferrous Metals Society of China **18**, 512-517 (2008).